A Discussion of
Radio Wavelength Radiation Generated by
Gyrosynchrotron and Langmuir-wave Processes

R. D. Robinson

Sacramento Peak Observatory, Sunspot, New Mexico 88349 U.S.A.

Abstract

Synchrotron and Langmuir-wave emission processes are compared, with special emphasis being placed on metre wavelength radiation from the solar corona. Numerical calculations are presented which relate to brightness temperature, circular polarization and source structure. It is found that both gyrosynchrotron and Langmuir processes can produce brightness temperatures up to ~ 2–3 GK; larger temperatures require induced Langmuir-wave emission. It is further shown that gyrosynchrotron source positions observed at different frequencies may have a dispersion in height within an inhomogeneous background medium. Although many observations may be explained exclusively by one of the two processes, there are numerous circumstances in which both processes are equally likely.

1. Introduction

Nonthermal radio waves can be generated by a number of physical processes, depending on the conditions within the source. In the chromosphere and corona of the Sun and stars, the two principal emission processes are gyrosynchrotron radiation and Langmuir waves.

Gyrosynchrotron radiation is produced when energetic charged particles spiral in a magnetic field. This emission process has been the subject of extensive study and is theoretically well understood (see e.g. Ginzburg and Syrovatskii 1965, 1969; Melrose 1968; Ramaty 1969). In the present paper I have computed the synchrotron radiation from mildly relativistic particles under solar coronal conditions. The formulae used are those given by Ramaty (1969), corrected according to the comments of Trulsen and Fejer (1970). These formulae are complex and must be solved numerically.

Langmuir waves are electrostatic disturbances created by electrons travelling more rapidly than the phase velocity of the wave. They have a frequency slightly larger than the local plasma frequency ω_p (where $\omega_p^2 = 4\pi n_e q^2/m$). A discussion of their generation and the wavenumber spectrum produced by various types of particle distributions has been given by Robinson (1978a). These waves can be converted to electromagnetic radiation by scattering on the electron clouds surrounding the ions or by the coalescence of two waves travelling in nearly opposite directions (see Ginzburg and Zhelezyniakov 1958; Melrose 1970a, 1970b, 1974a, 1974b; Smith 1970; Tsytovich 1970; Melrose and Sy 1972a, 1972b). These two conversion processes produce electromagnetic radiation at nearly the plasma frequency (called fundamental radiation) and at twice the plasma frequency (second harmonic radiation) respectively.

The present discussion focuses primarily on the brightness temperature, circular polarization and source structure expected from each of the two nonthermal emission mechanisms. Numerical calculations are presented which are applicable to metre wavelength radiation generated in the solar corona. In these calculations a wide range of source magnetic-field strengths and of thermal and nonthermal electron densities is considered. Two representations for the nonthermal electron energy distribution are used:

The first of these energy distributions is the 'power law', which has a momentum p dependence given by $f(p) \approx p^{-a}$. This distribution has been postulated for a large variety of solar bursts (e.g. Takakura 1972) and is often measured at the Earth's orbit by satellite (e.g. Svestka 1976). The second distribution, termed a 'gap' distribution by Melrose (1975), is characterized by a narrow range of energies centred about an energy E_0. Such a distribution may be produced in an electron beam when faster particles are able to outrun the slower (Magelssen and Smith 1977). It may also be produced within a magnetic trap if low energy electrons escape more quickly than the high energy electrons (Robinson 1978b, present issue pp. 533–45). For numerical calculations presented in the present paper, I assume that the gap distribution is characterized by a gaussian centred at a specified energy.

A third distribution, termed a 'plateau', which has a nearly constant momentum dependence below a given momentum p_m but decreases rapidly for greater values of p, has emission properties that are intermediate between those of the gap and power-law distributions (Robinson 1978a). Radiation produced by this distribution is not considered here.

By comparing theoretical results with observation, the observer may sometimes be able to determine the physical conditions within the source, including the plasma density, the magnetic field strength, the number density and distribution of nonthermal particles, and the evolution of these parameters.

2. Brightness Temperatures

(a) Gyrosynchrotron Radiation

The brightness temperature of gyrosynchrotron radiation is dependent on the optical depth of the source and the number of the dominant harmonic. For an optically thin source the temperature rapidly increases with increasing magnetic field strength. It is also linearly dependent upon the column density of nonthermal particles. As the source becomes optically deep, the temperature becomes approximately independent of both the field strength and the nonthermal particle density. The energy density of emitted radiation is then essentially the kinetic temperature of the emitting electrons.

For most cosmic objects (e.g. radio galaxies) absorption can be neglected. However, for stellar atmospheres, the magnetic fields and nonthermal particle fluxes are often sufficient for the absorption to be extremely important (see e.g. Dulk (1973) or Robinson (1974) for a discussion of the absorption present in solar type IV radio bursts).

Fig. 1 shows examples of the absorption coefficient and emissivity for a typical electron distribution and a range of magnetic field strengths and background plasma densities. Table 1 summarizes the maximum brightness temperature possible for a number of particle energy distributions. In these calculations, field

strengths from $10\,\mu T$ to $2\,mT$ and nonthermal number densities from 10^5 to $10^{10}\,m^{-3}$ were considered; brightness temperatures requiring parameters outside this range were considered unrealistic within the corona. The main point is that temperatures in excess of $1\,GK$ are unlikely even under the most optimistic circumstances.

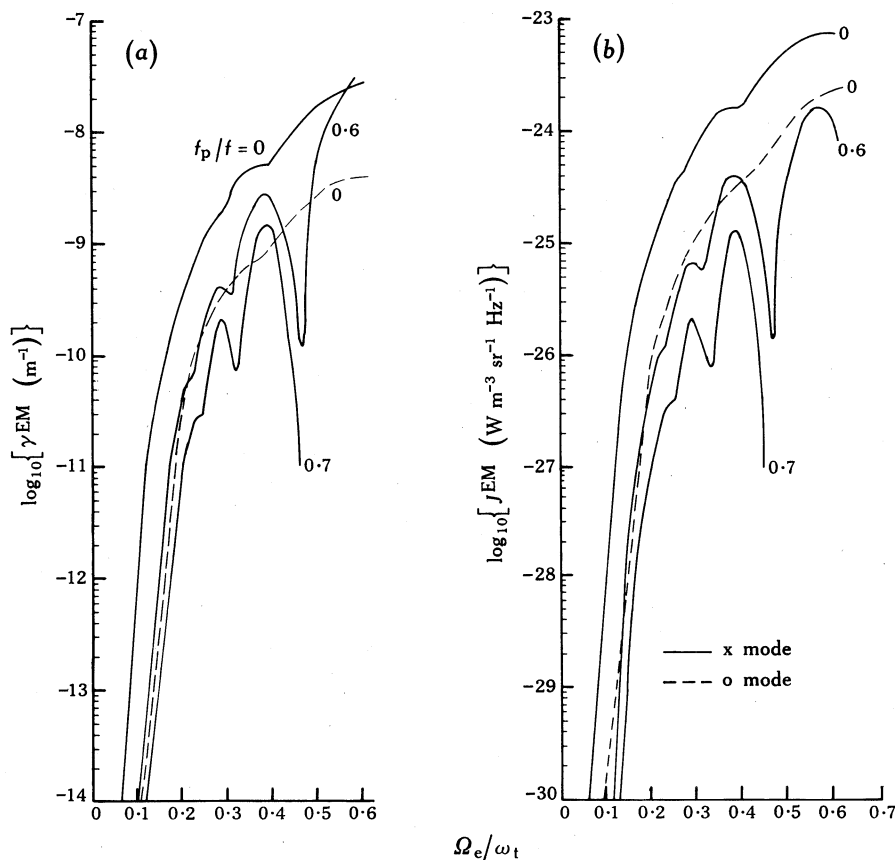**Fig. 1.** Variation with the normalized electron gyrofrequency Ω_e/ω_t of (a) the absorption coefficient γ^{EM} and (b) the emissivity J^{EM} for a gap energy distribution with central energy $E_0 = 100\,keV$, an e^{-1}-width of $10\,keV$ and an observation angle $\theta_{obs} = 50°$. Parameterization of the curves is by the indicated values of $\omega_p/\omega_t = f_p/f$.

(b) Langmuir Wave Emission

The brightness temperature of electromagnetic radiation generated from Langmuir waves depends greatly on the form and effective temperature of the Langmuir wave-number spectrum, as well as the structure of the ambient plasma. In an earlier paper (Robinson 1978a), I calculated the Langmuir wavenumber spectrum for a variety of electron distributions, and showed that electron distributions having an isotropic pitch-angle distribution produced stable (i.e. nongrowing) wavenumber spectra. The gap and plateau distributions produced spectra which were nearly constant over a wide range of wavenumbers, but which were limited in effective Langmuir-wave brightness temperatures $T_b^L(k)$ to values less than $10\,GK$. The

Table 1. Peak brightness temperatures for different electron distributions

The Lorentz factor γ_c determines the energy of the gap distribution peak and the power-law distribution cutoff, the gap-distribution energy width Δ represents the energy spread relative to the central energy E_0, and ε is the power-law negative index

γ_c	Δ	T_b^{max} (GK) for a frequency of:			
		40 MHz	80 MHz	160 MHz	320 MHz
		(a) Gaussian distribution			
1·2	0·3	0·16	0·16	0·16	0·16
1·2	0·5	0·17	0·17	0·17	0·17
2·0	0·1	0·56	0·56	0·56	0·57
2·0	0·3	0·55	0·55	0·55	0·55
2·0	0·5	0·59	0·59	0·59	0·59
10·0	0·1	4·1	3·8	3·0	2·0
10·0	0·3	3·8	3·6	3·0	2·0
10·0	0·5	3·6	3·4	2·8	1·9
γ_c	ε	T_b^{max} (GK) for a frequency of:			
		40 MHz	80 MHz	160 MHz	320 MHz
		(b) Power-law distribution			
1·02	4	0·08	0·10	0·0020	—
1·2	2	1·0	0·82	0·64	0·48
1·2	4	0·24	0·22	0·21	0·20
1·2	8	0·16	0·16	0·16	0·16
2·0	4	0·65	0·65	0·64	0·64
2·0	8	0·57	0·57	0·57	0·57

effective brightness is defined such that $KT_b^L(k)$ is the energy density of Langmuir waves at wavenumber k (see e.g. Melrose 1974a), K being the Boltzmann constant.

When electrons undergo streaming, are trapped in a magnetic mirror or are formed into other anisotropic pitch-angle distributions, there is the possibility of induced emission of Langmuir waves (i.e. the distribution becomes unstable). When this occurs extremely large Langmuir-wave brightness temperatures are possible. Unstable electron distributions will have an exponentially increasing Langmuir-wave brightness temperature, and the final spectrum will depend upon the detailed evolution of the electron distribution. I have calculated elsewhere (Robinson 1978a) the rate of wave growth (specified by the parameter $\gamma(k)$) for a variety of energy and pitch-angle distributions and have shown that the growth generally reaches a sharp maximum for some wavenumber, in most cases near the low wavenumber end of the spectrum. Calculations describing the detailed evolution of the electron distribution and the emitted Langmuir wavenumber spectrum are beyond the scope of the present paper and have not been attempted. Instead, to study the possible electromagnetic radiation from a source containing an unstable electron distribution, I have postulated that the final Langmuir wavenumber spectrum peaks at the low wavenumber end of the spectrum. The form of the spectrum assumed is

$$T_b^L(k) = T_b^{max} \exp\left(-(k-k_{min})/k_0\right) \qquad k > k_{min}, \qquad (1a)$$

$$= 0 \qquad\qquad\qquad\qquad\qquad k < k_{min}, \qquad (1b)$$

where $k_{min} = 0 \cdot 033$ and corresponds to resonance with 100 keV electrons, while T_b^{max} and k_0 are the peak brightness temperature of the spectrum and the rate of decrease toward high wavenumbers respectively.

The brightness temperature T^{EM} of the electromagnetic radiation was determined from the spectrum (1) using the radiative transfer formula

$$\partial(KT^{EM})/\partial x = J^{EM} - \gamma^{EM} KT^{EM}, \tag{2}$$

where J^{EM} is the coefficient of spontaneous emission and γ^{EM} is the 'absorption coefficient'. In all numerical calculations the assumed coronal density distribution was that given by Newkirk (1967) for a coronal streamer, and the transfer calculations were conducted only along the density gradients, so that refraction of the waves could be ignored. For fundamental radiation, equation (2) was solved for all plasma levels having plasma frequency ω_p less than the frequency of the observed electromagnetic radiation ω_t. For second-harmonic radiation, the solution was obtained for $\omega_p < \frac{1}{2}\omega_t$.

Expressions for the emission and absorption coefficients have been given by, among others, Melrose (1974a). For the fundamental, the absorption coefficient is given as

$$\gamma_F^{EM} = \frac{\pi}{3(2\pi)^{5/2}} \frac{\omega_p^2}{n_i v_i} \frac{1}{v_g^{EM}} \int_{k_{min}}^{k_{max}} \frac{k_L(\omega_t - \omega_L)}{\omega_L} \exp\left(-\frac{1}{2}\{(\omega_L - \omega_t)/k_L v_i\}^2\right) \chi \frac{T^L(k_L)}{T_i} dk_L, \tag{3a}$$

where v_g^{EM} is the group velocity of the observed electromagnetic radiation, ω_L and k_L are the frequency and wavenumber of the Langmuir waves, n_i and v_i are the number density and thermal velocity of the ambient ions, and k_{max} and k_{min} are the limits of the Langmuir wavenumber spectrum.

For the second harmonic the absorption coefficient is given by

$$\gamma_H^{EM} = 0 \cdot 02 \frac{r_0 \omega_p^2}{c^2} \frac{c}{V_{th}} \left(\frac{\omega_t - 2\omega_p}{2\omega_p}\right)^{\frac{1}{2}} \frac{KT_b^L(k_R)}{KT_{th}}, \tag{3b}$$

where $r_0 \ (= q^2/m_0 c^2)$ is the classical electron radius, T_{th} is the temperature of the ambient plasma and k_R is the wavenumber required at a given plasma level for two Langmuir waves to coalesce and produce an electromagnetic wave:

$$k_R = \{(\omega_t - 2\omega_p)\omega_p/3V_{th}^2\}^{\frac{1}{2}}. \tag{4}$$

There can be no induced emission (negative absorption) of second-harmonic radiation, since the absorption coefficient of equation (3b) is positive for all plasma levels. Consideration of the absorption coefficient of equation (3a), however, shows that there is a possibility for negative absorption over a range of coronal heights provided waves with $\omega_L > \omega_t$ dominate in the integral. Over this region the brightness temperature increases exponentially, the rate of increase being dependent on the size of the absorption coefficient. This amplification region extends above the level for which $\omega_t = \omega_p$ and covers a length L_F of corona given approximately by (Melrose 1974a)

$$L_F = \frac{3}{2}\omega_t \frac{V_{th}^2}{V_\phi^2} \Big/ \left(\frac{\partial \omega_p}{\partial z}\right)_{\omega_p = \omega_t}, \tag{5}$$

where z is the length variable measured parallel to the density gradient and V_ϕ ($= \omega_L/k_L$) is the phase velocity of the Langmuir wave. Above the amplification region, the absorption coefficient becomes positive and the waves are damped. The important point to notice is that L_F is strongly dependent on the value of V_ϕ, and therefore on the wavenumber at which the plasma spectrum peaks. Since the final brightness temperature depends exponentially on the amplification distance, it is possible that Langmuir waves having larger k values (even if they have smaller effective temperatures) may dominate for the case of a broad Langmuir wavenumber spectrum.

Table 2. Brightness temperatures for different electron distributions and wavenumber spectra

$T^L_{b,max}$, T^F_b and T^H_b are the maximum brightness temperature of the Langmuir waves and the fundamental and second-harmonic brightness temperatures respectively, while τ^F_{tot} and τ^H_{tot} are the total optical depths from the plasma level outwards for fundamental and second-harmonic radiation (the optical depth values being determined by numerical radiative transfer techniques)

E_0 (keV)	Δ	n_e (m^{-3})	$T^L_{b,max}(k)$ (GK)	$T^F_b(k)$ (GK)	$\tau^F_{tot}(k)$ (10^{-3})	$T^H_b(k)$ (GK)	$\tau^H_{tot}(k)$ (10^{-3})
			(a) Gap energy distribution model				
10	0·1	10^9	15	0·22	−2	0·0054	0·71
25	0·1	10^9	10	0·20	−1·9	0·0047	0·63
100	0·01	10^9	3	0·060	−0·4	0·00018	0·58
100	0·1	10^9	6	0·14	−0·9	0·00096	0·14
100	0·1	10^8	6	0·11	−0·7	0·00069	0·11
100	0·1	10^7	6	0·014	−0·35	0·00034	0·077
500	0·1	10^9	7	0·15	−0·8	0·00087	0·12
1000	0·1	10^9	9	0·24	−1·0	0·00075	0·11

k_0	$T^L_{b,max}(k)$ (GK)	$T^F_b(k)$ (GK)	$\tau^F_{tot}k)$ (10^{-3})	$T^H_b(k)$ (GK)	$\tau^H(k)$ (10^{-3})
	(b) Peaked Langmuir wavenumber spectrum model (equation 1)				
0·02	10	0·060	−0·14	—	—
0·02	10^4	58	−120	1·6	4·6
0·02	10^6	4·5×10^9	−12·2×10^4	1·2×10^5	4600
0·01	10	—	—	2·8×10^{-5}	8·3×10^{-3}
0·01	10^4	32	−47	5·2	1·3
0·01	10^6	2·4×10^4	−4700	4·8×10^4	130
0·005	10	0·016	−0·038	5·4×10^{-6}	5·0×10^{-3}
0·005	10^4	16	−1·3	1·7	0·43
0·005	10^6	1300	−1700	1·6×10^4	43
0·0025	10	0·016	−0·038	—	—
0·0025	10^4	6·4	−5·2	0·33	0·13
0·0025	10^6	410	−500	3300	13

Table 2 summarizes the results of the numerical radiation transfer calculations. Included in the table is the optical depth of the source region.

In the majority of cases the source optical depths are small. The brightness temperature is then primarily dependent on the length of corona over which conversion is possible and the value of the emission coefficient. Emissivity for the

fundamental is linearly dependent on the Langmuir wave brightness, while that for the harmonic is dependent on the square of the Langmuir wave brightness (Melrose 1974a). The harmonic is therefore more sensitive to the parameters of the Langmuir wavenumber spectrum than is the fundamental. This fact is evident from Table 2.

For low temperatures of Langmuir waves ($T_b^L < 10\,\mathrm{GK}$), production of the harmonic is ineffective and the fundamental will dominate. As the Langmuir wave temperature is increased, the harmonic brightness will also increase and can become comparable with the fundamental brightness. The conditions required for the harmonic to dominate depend upon both the width and temperature of the Langmuir spectrum. As the Langmuir wave temperature is further increased, induced effects become important and fundamental radiation with brightness temperature in excess of the Langmuir temperature is produced (Smith and Sturrock 1971). The harmonic temperature, however, is restricted to values less than those of the Langmuir waves.

Table 2a presents calculations for well-determined Langmuir wave spectra, i.e. spectra produced by stable electron distributions (Robinson 1978a). However, the values in Table 2b were calculated on the basis of the assumed spectra in equation (1) and are not well suited to the determination of the region where the harmonic emission dominates the fundamental. As mentioned earlier, the harmonic is very sensitive to the plasma wave spectrum, and small changes in the development of the source could greatly change the values listed. The main purpose of the table is to illustrate fundamental and harmonic brightness variations as related to changes in the Langmuir wavenumber spectrum.

While the results of Table 2 illustrate the magnitude of the temperature obtainable under a variety of circumstances, it should be mentioned that there are a number of variables which could change the observed temperature. Changes in the density gradients of the background plasma, small- and large-scale density inhomogeneities within the source, a nonisotropic distribution of Langmuir waves, as well as refraction of the ray paths would all act to change the amplification distance and therefore change the observed brightness temperature. The effects of these and other parameters have been discussed by Melrose (1974a) and Robinson (1977).
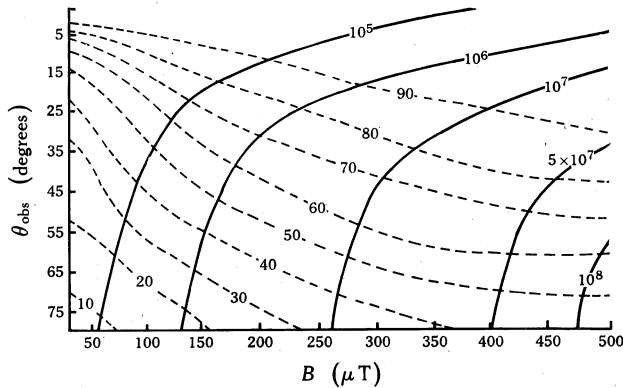
3. Circular Polarization

(a) Synchrotron Radiation

The circular polarization of synchrotron radiation is dependent upon the angle of the magnetic field with respect to the observation direction and the optical-depth properties of the source. The extraordinary magnetoionic mode (x-mode) emission coefficient is considerably larger than the coefficient for the ordinary mode (o-mode). Thus, for an optically thin source, the polarization will always be in the extraordinary sense.

The degree of polarization depends on the particle energy and magnetic field present. Kai (1969) pointed out that polarizations of 80%–90% sometimes seen in moving type IV solar radio bursts must be explained by radiation from mildly relativistic particles. This is due to the fact that low energy particles emit primarily into low harmonics, which have a high degree of polarization. Increasing the energy

produces larger contributions to the higher harmonics, which are less polarized (Bekefi 1966). As the average energy of the particles increases, the o-mode intensity grows in relation to the x-mode, while the net polarization decreases. We do not expect a complete absence of polarization under coronal conditions, however, even for electrons with an energy of 10 MeV or greater.

Fig. 2. Contours of constant brightness temperature T_b in kelvins (solid curves) and percentage circular polarization P (dashed curves) in the magnetic field – observation angle plane. The assumed electron energy distribution has the form $N(E) \propto E^{-2}$ for $10 < E < 100$ keV and $N(E) \propto E^{-4}$ for $E > 100$ keV. The assumed nonthermal particle density is 10^9 m^{-3}. The optical depth is less than unity over the entire plot.

Fig. 2 shows the effect of the magnetic field strength and the observation angle on the polarization of an optically thin synchrotron source. As the average energy of the emitting electrons increases, the polarization at each point will decrease. However, the basic form of the figure is representative of the behaviour for most sources. The main point to notice is that high values of circular polarization are restricted to large fields and low angles of observation.

Because the x-mode absorption coefficient is larger than the o-mode (Fig. 1), the source will initially become optically deep and saturate in the extraordinary mode as the magnetic field and/or the number density of emitting electrons increase. For further increases in field strength or number density there will be a relative increase of o-mode brightness until it saturates also. Since the ordinary mode has a larger source function than the extraordinary, the final polarization of an optically thick homogeneous source will be in the o-mode sense. This has been shown for mildly relativistic electrons by Ramaty (1969) and Dulk (1973) and for ultrarelativistic particles by Melrose (1968). For an optically thick inhomogeneous source the x-mode and o-mode radiation will originate from different regions within the source (Robinson 1974). If we assume that the source decreases in magnetic field strength away from the centre, a nearly unpolarized source results.

(b) Polarization from Langmuir Wave Processes

In the presence of a weak magnetic field, the conversion process from Langmuir to electromagnetic waves produces approximately equal amplitudes of the ordinary

and extraordinary magnetoionic waves (Melrose and Sy 1972*a*). If both modes were allowed to escape, there would be only small degrees of circular polarization observed. However, while the ordinary mode will propagate for all plasma frequencies for which $\omega_t > \omega_p$, the extraordinary mode is restricted to $\omega_t > \omega_x$ (Melrose and Sy 1972*b*), where

$$\omega_x = \tfrac{1}{2}\Omega_e + \tfrac{1}{2}(4\omega_p^2 + \Omega_e^2)^{\frac{1}{2}} \approx \omega_p + \tfrac{1}{2}\Omega_e \qquad (6)$$

in the weak field limit ($\omega_p \gg \Omega_e$), with Ω_e the electron gyrofrequency (rad s^{-1}). All x-mode radiation produced between $\omega_p = \omega_t$ and $\omega_t - \tfrac{1}{2}\Omega_e$ is prevented from escaping and o-mode polarization will result. The degree of polarization depends on the amount of wave generation between the two levels.
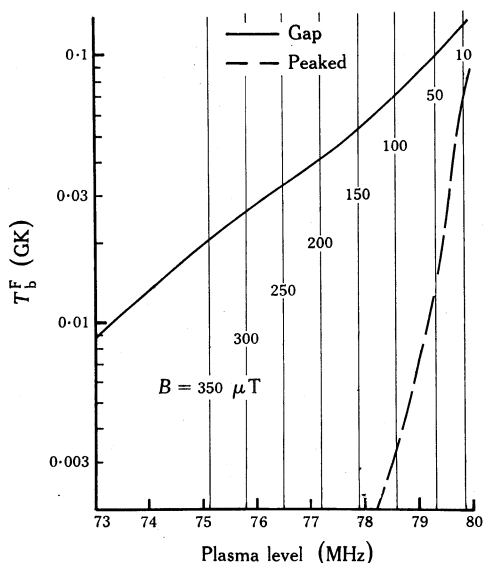

Fig. 3. Results of numerical radiative-transfer calculations for the production of fundamental radiation, showing the variation with the plasma level of the brightness temperature T_b^F for the Langmuir wavenumber spectra produced by a gap distribution (Robinson 1978*a*) and the peaked spectrum (equation 1) as indicated. The cutoff levels for x-mode radiation are shown with indicated magnetic field strengths B. The assumed observation frequency is 80 MHz.

Fig. 3 shows the results of a numerical radiation transfer for the fundamental, using both a broad Langmuir spectrum characteristic of the gap distribution and a sharply peaked spectrum as expected for unstable distributions (see equation 1). Plotted against the plasma level is the integrated contribution to the brightness temperature from all plasma levels at greater heights than the level plotted. For the ordinary mode, the total observed brightness temperature is that plotted at $\omega_p = \omega_t = 80$ MHz in this case. For the extraordinary mode, only that temperature at $\omega_p = 80 - \tfrac{1}{2}\Omega_e$ will be seen. It is apparent that the x-mode temperature for the sharply peaked spectrum is considerably more sensitive to the field strength than is that for the broad spectrum.

Table 3 gives the calculated polarizations in the two cases and shows that, while the highly peaked spectrum produced 100% o-mode polarization for field strengths greater than 20 μT (agreeing with Melrose and Sy 1972*b*), the broad spectrum requires strengths of 100 μT before appreciable polarization is evident. This may be a partial explanation for the low polarizations observed in many solar events.

The emission at the harmonic is not influenced by x-mode cutoff levels, and low degrees of polarization are expected (Melrose and Sy 1972*b*). While the levels of emitted x-mode and o-mode waves are approximately equal for low field strengths,

emission preferences occur as the field strength increases. Melrose *et al.* (1978), using the analysis of Melrose and Sy (1972*b*), calculated the dependence of polarization on field strength and found that appreciable x-mode emission can occur.

Table 3. Polarization variation for different electron distributions and wavenumber spectra

P^F is the percentage circular polarization of the fundamental radiation expected from the indicated ambient magnetic fields (assumed to be homogeneous)

E_0 (keV)	Δ	P^F (%) for a magnetic field strength of:			
		$10\,\mu$T	$50\,\mu$T	$100\,\mu$T	$200\,\mu$T
(a) Gap distribution model with pitch-angle isotropy					
10	0·1	0	0	0	6
25	0·1	0	0	9	26
100	0·01	1	19	33	51
100	0·1	4	21	36	58
500	0·1	5	30	45	63
1000	0·1	7	36	53	70

| k_0	P^F (%) for a magnetic field strength of:			
	$10\,\mu$T	$50\,\mu$T	$100\,\mu$T	$200\,\mu$T
(b) Peaked wavenumber spectrum model (equation 1)				
0·005	11	100	100	100
0·01	8	89	100	100
0·02	7	72	90	100

4. Source Structure

Since the radiation generated by the conversion of Langmuir waves originates very near the local plasma level, it is expected that sources at different frequencies will be spread over a range of heights corresponding to the spread in plasma frequencies. This, indeed, has been shown to be the case in such Langmuir-wave sources as solar type III radio bursts and continuum storms (Magun *et al.* 1975; Stewart 1976). The *observed* source locations, however, do not exactly correspond to the plasma levels because of the refraction and scattering of the radiation as it escapes from the plasma (see e.g. Riddle 1972, 1974; Leblanc 1973).

Synchrotron radiation in a vacuum or from a very compact source will yield overlapping source positions at different frequencies. The source location will depend on the location of the largest magnetic field strengths and greatest density of nonthermal particles. When synchrotron radiation is generated over a large area in an inhomogeneous plasma (such as within a magnetic arch in the solar corona) there will be two competing processes tending to limit the observed size and location of the source. The first is Razin suppression, which restricts the radiation to heights in which the plasma frequency is less than $\omega_p \approx \omega_t \Omega_e$ (Melrose 1972; Wild and Hill 1971). The second effect is the decrease in magnetic field strength with height, which causes a consequent decrease in the emission and absorption coefficients with height. For an optically thin source, this decrease in emissivity results in a rapid decrease in brightness; while for an optically thick source there will be a decrease in optical depth. The upper boundary of the source is then determined either by the

decrease in brightness, for an optically thin source; or by the height at which the optical depth is less than 1, for an optically thick source.

The two selection processes are frequency dependent and cause a natural dispersion of source heights. The high frequencies come from lower depths of the corona, due to the greater plasma density required for Razin suppression (fixing the lower boundary of the source) and the smaller emission and absorption coefficients at a given magnetic field strength (fixing the upper boundary).
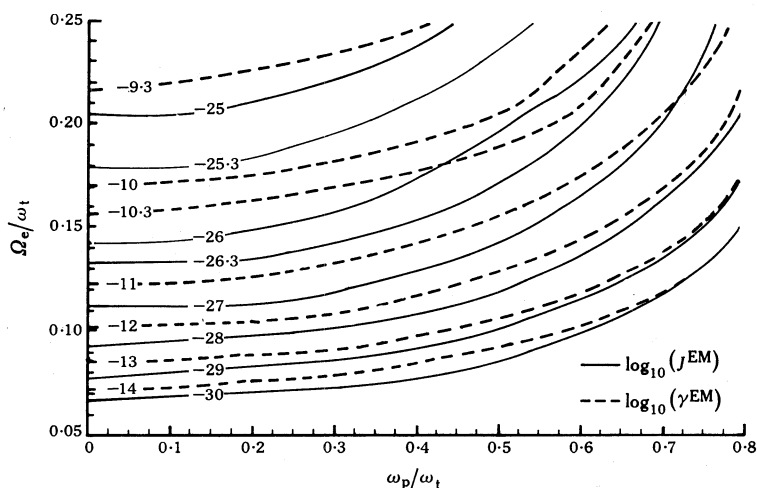
Fig. 4. Contours of constant emissivity (solid curves labelled as $\log_{10}(J^{EM})$ in $W\,m^{-3}\,sr^{-1}\,Hz^{-1}$) and absorption coefficient (dashed curves labelled as $\log_{10}(\gamma^{EM})$ in m^{-1}) on the normalized plasma frequency – electron gyrofrequency plane for a gaussian gap distribution centred at 100 keV. For a homogeneous source, the total absorption is given as $\tau = \gamma^{EM} NL$, where γ^{EM} is the absorption coefficient, N is the number density of nonthermal particles (m^{-3}) and L is the source thickness (m), while the total emissivity is $J^{EM} = \varepsilon^{EM} NL$, where ε^{EM} is the emission coefficient presented. For low optical depths, the observed brightness temperature is $T_p = \frac{1}{2}\lambda^2 J^{EM}/K$ kelvin, where λ is the observed wavelength (m).

To get a more quantitative idea of the source production process consider Fig. 4, which gives contours of constant emissivity and absorption in a $\Omega_e/\omega_t, \omega_p/\omega_t$ plane for a gap distribution of energetic electrons. The radiation from a source can be estimated using this diagram by plotting the values for Ω_e and ω_p within the source and then determining the brightness temperature.

To model the source structure, it is necessary to specify a magnetic field strength for each plasma level. Three such models are plotted in Figs 5a, 5c and 5e, and the resultant variations in the height of the emission and absorption coefficients, derived using Fig. 4, are shown in Figs 5b, 5d and 5f. Note the source dispersion with height, the width of the distribution and the maximum emissivity with frequency, and how these properties vary as the model is changed.

5. Conclusions

Radio wavelength observations can act as an important probe into the physical conditions within a source. Occasionally it is possible to positively specify the emission process. Langmuir wave generation is definitely indicated if the radiation
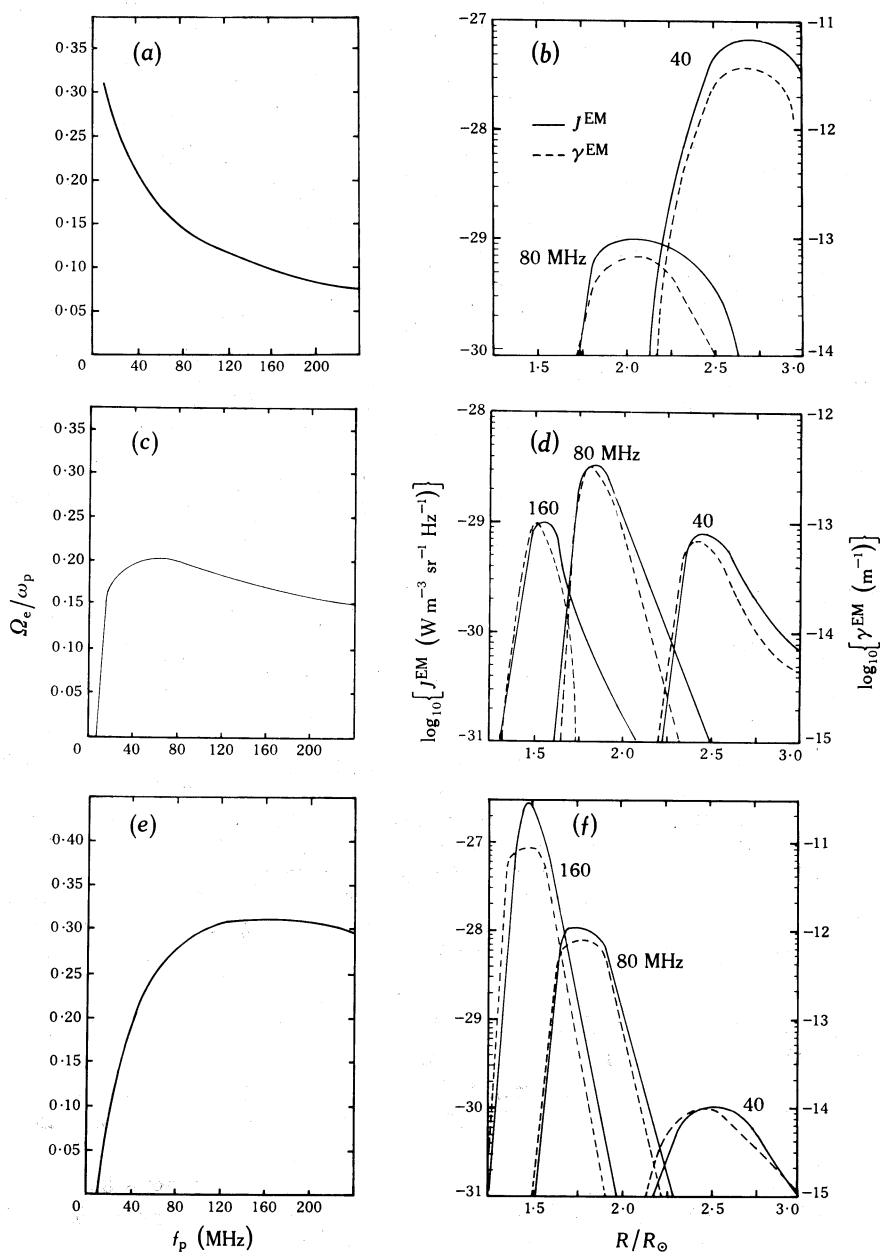
Fig. 5. Models of synchrotron sources in inhomogeneous media (based on the emission and absorption data of Fig. 4) together with predicted source structures. The models (*a*, *c* and *e*) are specific forms for the variation of the normalized electron gyrofrequency Ω_e/ω_p as a function of the magnetic field plasma frequency f_p (as described in the text). The representative source structures (*b*, *d* and *f*) are variations of the emissivity J^{EM} and the absorption coefficient γ^{EM} with the radial height $R/R_\odot$ normalized to the solar radius. As long as the optical depth is less than unity for all heights, the brightness temperature distribution will pattern the emissivity.

has a very narrow wavelength range (fine structure) emission at a fundamental and second harmonic (e.g. as in solar type III and type II events), large brightness temperatures (>10 GK) or is strongly polarized in the ordinary sense (as for solar continuum storms). The fine structure may be produced by direct conversion of Langmuir waves (e.g. as in type I bursts; Sy 1973) or by coalescence with other wave modes (Rosenberg 1972; Chiuderi *et al.* 1973). Synchrotron radiation, on the other hand, is indicated if the source appears well above the plasma level, has a large bandwidth with little narrow-bandwidth fine structure, or can be deduced as coming from an electron distribution which is a steeply decreasing function of energy.

It is evident from the results of this paper that many observations can be explained by either emission process. For example, observed brightness temperatures less than 10 GK, a dispersion of source heights and a moderate or small polarization can be explained equally well by plasma or synchrotron processes.

Occasionally it is possible to determine the process by study of the time evolution of the various parameters. For example, since the polarization and brightness temperature of synchrotron radiation are closely linked through the source optical depth, an increase in polarization accompanying the decay of the source would generally indicate synchrotron emission. Langmuir wave sources, however, have a polarization relatively independent of the brightness temperature. A constant polarization during the declining phase of the burst may therefore indicate Langmuir radiation.

Once the radiation mechanism is determined it is possible to use the observations to specify some physical parameters of the source. For Langmuir wave emission, the brightness temperature and polarization are primarily dependent upon the electron distribution and the magnetic field respectively. The density and distribution of the ambient plasma are then determined by study of the frequency spread and the source structure (after taking account of refraction and scatter within the corona; see Riddle 1972, Stewart 1976).

For synchrotron radiation the polarization, temperature and source structure are interrelated and all depend upon a large number of variables. However, by making certain assumptions based upon other observations it is often possible to derive a number of source parameters and their evolution. As an example, Dulk (1973) and Robinson (1974) have studied the synchrotron radiation from moving type IV solar radio bursts. By assuming a power law energy distribution, which seems reasonable based upon microwave observations (Takakura 1972), it was possible to deduce an empirical model for the evolution of the magnetic field and number density of nonthermal electrons as the source evolved.

References

Bekefi, G. (1966). 'Radiation Processes in Plasmas' (Wiley: New York).

Chiuderi, C., Giachetti, R., and Rosenberg, H. (1973). *Solar Phys.* **33**, 225.

Dulk, G. A. (1973). *Solar Phys.* **32**, 491.

Ginzburg, V. L., and Syrovatskii, S. I. (1965). *Annu. Rev. Astron. Astrophys.* **3**, 297.

Ginzburg, V. L., and Syrovatskii, S. I. (1969). *Annu. Rev. Astron. Astrophys.* **7**, 375.

Ginzburg, V. L., and Zhelezyniakov, V. V. (1958). *Sov. Astron. AJ* **2**, 653.

Kai, K. (1969). *Proc. Astron. Soc. Aust.* **1**, 189.

Leblanc. Y. (1973). *Astrophys. Lett.* **14**, 41.

Magelssen, G. R., and Smith, D. F. (1977). *Solar Phys.* **55**, 211.

Magun, A., Stewart, R. T., and Robinson, R. D. (1975). *Proc. Astron. Soc. Aust.* **2**, 367.

Melrose, D. B. (1968). *Astrophys. Space Sci.* **2**, 171.

Melrose, D. B. (1970a). *Aust. J. Phys.* **23**, 871.

Melrose, D. B. (1970b). *Aust. J. Phys.* **23**, 885.

Melrose, D. B. (1972). *Astrophys. Space Sci.* **18**, 267.

Melrose, D. B. (1974a). *Solar Phys.* **35**, 441.

Melrose, D. B. (1974b). *Aust. J. Phys.* **27**, 259.

Melrose, D. B. (1975). *Solar Phys.* **43**, 211.

Melrose, D. B., Dulk, G. A., and Smerd, S. F. (1978). *Astron. Astrophys.* **66**, 315.

Melrose, D. B., and Sy, W. N. (1972a). *Astrophys. Space Sci.* **17**, 343.

Melrose, D. B., and Sy, W. N. (1972b). *Aust J. Phys.* **25**, 387.

Newkirk, G., Jr (1967). *Annu. Rev. Astron. Astrophys.* **5**, 213.

Ramaty, R. (1969). *Astrophys. J.* **158**, 753.

Riddle, A. C. (1972). *Proc. Astron. Soc. Aust.* **2**, 98.

Riddle, A. C. (1974). *Solar Phys.* **34**, 181.

Robinson, R. D. (1974). *Proc. Astron. Soc. Aust.* **2**, 258.

Robinson, R. D. (1977). Ph.D. Thesis, University of Colorado.

Robinson, R. D. (1978a). *Astrophys. J.* **222**, 696.

Robinson, R. D. (1978b). *Aust. J. Phys.* **31**, 533.

Rosenberg, H. (1972). *Solar Phys.* **25**, 188.

Smith, D. F. (1970). *Adv. Astron. Astrophys.* **7**, 148.

Smith, D. F., and Sturrock, P. A. (1971). *Astrophys. Space Sci.* **12**, 411.

Stewart, R. T. (1976). *Solar Phys.* **50**, 437.

Svestka, Z. (1976). 'Solar Flares' (Reidel: Dordrecht, Holland).

Sy, W. N. (1973). Ph.D. Thesis, Australian National University.

Takakura, T. (1972). *Solar Phys.* **26**, 151.

Trulsen, J., and Fejer, J. A. (1970). *Plasma Phys.* **4**, 825.

Tsytovich, V. N. (1970). 'Non-Linear Effects in Plasmas' (Plenum: New York).

Wild, J. P., and Hill, E. R. (1971). *Aust. J. Phys.* **24**, 43.